THE JOURNAL OF BIOLOGICAL CHEMISTRY VOL. 287, NO. 39, pp. 32630–32639, September 21, 2012

Identification of Protein Interfaces between α-Synuclein, the Principal Component of Lewy Bodies in Parkinson Disease, and the Molecular Chaperones Human Hsc70 and the Yeast Ssa1p*

Received for publication, June 5, 2012, and in revised form, July 24, 2012 Published, JBC Papers in Press, July 26, 2012, DOI 10.1074/jbc.M112.387530

Virginie Redeker[‡1], Samantha Pemberton[‡1], Willy Bienvenut[§], Luc Bousset[‡], and Ronald Melki[‡2]

From the [‡]Laboratoire d'Enzymologie et Biochimie Structurales, CNRS, 91198 Gif-sur-Yvette, France and [§]Centre de Recherche de Gif, FRC3115, CNRS, 91198 Gif-sur-Yvette, France

Background: The mechanism by which molecular chaperones sequester α-synuclein is unknown.
Results: We identify the surface interfaces involved in Hsc70 and Ssa1p interaction with α-synuclein.
Conclusion: Hsc70 and Ssa1p bind α-synuclein like a tweezer through the two tips of their client protein binding sites.
Significance: Elucidating how molecular chaperones bind proteins involved in neurodegenerative diseases is relevant to design therapeutic tools.

Fibrillar α-synuclein (α-Syn) is the principal component of Lewy bodies, which are evident in individuals affected by Parkinson disease (PD). This neuropathologic form of α-Syn plays a central role in PD progression as it has been shown to propagate between neurons. Tools that interfere with α-Syn assembly or change the physicochemical properties of the fibrils have potential therapeutic properties as they may be sufficient to interfere with and/or halt cell-to-cell transmission and the systematic spread of α-Syn assemblies within the central nervous system. Vertebrate molecular chaperones from the constitutive/heat-inducible heat shock protein 70 (Hsc/p70) family have been shown to hinder the assembly of soluble α-Syn into fibrils and to bind to the fibrils and very significantly reduce their toxicity. To understand how Hsc70 family members sequester soluble α-Syn, we set up experiments to identify the molecular chaperone-α-Syn surface interfaces. We cross-linked human Hsc70 and its yeast homologue Ssa1p and α-Syn using a chemical cross-linker and mapped the Hsc70- and Ssa1p-α-Syn interface. We show that the client binding domain of Hsc70 and Ssa1p binds two regions within α-Syn similar to a tweezer, with the first spanning residues 10–45 and the second spanning residues 97–102. Our findings define what is necessary and sufficient for engineering Hsc70- and Ssa1p-derived polypeptide with minichaperone properties with a potential as therapeutic agents in Parkinson disease through their ability to affect α-Syn assembly and/or toxicity.

Various factors, including genetic susceptibility and environmental influences, can trigger the assembly of the protein α-synuclein (α-Syn)[3] from its soluble state into fibrils with high β-sheet content (1, 2). The latter form is one of the principal components of intracellular Lewy bodies, whose presence in the central nervous system is a defining feature of Parkinson disease (PD) and other synucleinopathies (3). Indeed, symptoms of PD are apparent after >70% of dopaminergic termini and/or neurons have been lost, with some of the remaining neurons containing filamentous α-Syn.

We and others (4–6) recently contributed evidence for intercellular propagation of α-Syn assemblies *in vivo*. This process has been proposed to contribute to the progressive spreading of α-synucleinopathies throughout the nervous system (7, 8). Thus, tools that inhibit α-Syn assembly into fibrils, which we recently showed to be the most toxic species (9), or change the physicochemical properties of the fibrils in such a way that the cell-to-cell propagation of α-Syn aggregates is affected, are most likely expected to have therapeutic potential in PD.

Molecular chaperones facilitate the folding of newly synthesized polypeptides (10). They also inhibit the aggregation of misfolded and stress-induced unfolded proteins by binding to exposed hydrophobic regions on non-native proteins and holding the proteins (11, 12). The expression of members of the Hsp70 family (13–16) is induced when a cellular environment is under stress such as heat shock, ischemia, or other stresses (17). This prompted us and others to document the effect of Hsc/p70 on α-Syn assembly *in vitro* and *in vivo* (18, 19). Hsc/p70 have been shown to inhibit α-Syn fibril formation. Furthermore, a reduction in the toxicity of fibrillar α-Syn upon coating the fibrils with Hsc70 was observed. These findings encouraged us to consider the use of Hsc/p70 as a potential therapeutic tool in PD (18, 20).

Here, using chemical cross-linking with the homobifunctional NHS-ester BS2G, we show evidence for an Hsc70-α-Syn complex. We map the surface interface between Hsc70 and

* This work was supported by the French Ministry of Education, Research, and Technology; the Centre National de la Recherche Scientifique (CNRS) and the Institut National de la Santé et de la Recherche Médicale, the Era-Net Neuron, the Agence Nationale pour la Recherche (ANR-08-NEUR-001-01), the Fondation de France (Parkinson), and the Human Frontier Science Program.

[1] Both authors contributed equally to this work.

[2] To whom correspondence should be addressed: Laboratoire d'Enzymologie et Biochimie Structurales, CNRS, Avenue de la Terrasse, 91198 Gif-sur-Yvette, France. Tel.: 33-16-982-3503; Fax: 33-16-982-3129; E-mail: melki@lebs.cnrs-gif.fr.

[3] The abbreviations used are: α-Syn, α-synuclein; PD, Parkinson disease; BS2G, Bis [Sulfosuccinimidyl] glutarate.

α-Syn after identification of the cross-linked polypeptides by nanoLC-MS/MS LTQ-Orbitrap analyses.

As the introduction to the body of an endogenous protein as a therapeutic agent may evoke an autoimmune response as described (21–25), we also documented the interaction of a polypeptide that may have an effect on α-Syn assembly and/or the toxicity similar to Hsc70 although exogenous to the human body: the yeast homologue of Hsp70, Ssa1p.

We show here that similarly to Hsc/p70, Ssa1p inhibits α-Syn assembly by sequestering it in an assembly incompetent state. We determined the affinity of Ssa1p for α-Syn and show that the apparent dissociation constant is comparable to that we measured between human Hsc70 and soluble α-Syn. Finally, we show evidence for an Ssa1p-α-Syn complex using chemical cross-linking with the homobifunctional NHS-ester BS2G, and we map the surface interface between Ssa1p and α-Syn after identification of the cross-linked polypeptides by nanoLC-MS/MS LTQ-Orbitrap analyses.

EXPERIMENTAL PROCEDURES

Expression and Purification of α-Syn, Hsc70, and Ssa1p—Recombinant wild-type α-Syn was expressed in *Escherichia coli* strain BL21(DE3) (Stratagene) and purified as described (26). α-Syn concentration was determined spectrophotometrically using an extinction coefficient of 5960 $M^{-1}\cdot cm^{-1}$ at 280 nm. Pure α-Syn (0.5–1 mM) in 50 mM Tris-HCl, pH 7.5, 50 mM KCl was stored at −80 °C.

Recombinant hexahistidine tagged wild-type Hsc70 and Ssa1p (yeast strain AJYM28), were purified as described previously (18 and 27, respectively). Hsc70 and Ssa1p concentrations were determined by Bradford assay (28). Pure Hsc70 and Ssa1p (10–80 μM) in 50 mM Tris-HCl, pH 7.5, 150 mM KCl, 5 mM β-mercaptoethanol, 5 mM $MgCl_2$, 1 mM EGTA, and 10% glycerol were aliquoted and stored at −80 °C. To make sure that Hsc70 and Ssa1p are functional, their ATPase activities, alone or in the presence of α-Syn fibrils, was monitored as described (29) (data not shown).

Assembly of α-Syn into Fibrils—Soluble wild-type α-Syn was assembled in 50 mM Tris-HCl, pH 7.5, 150 mM KCl, in the absence or presence of Ssa1p, with or without ADP-$MgCl_2$ or ATP-$MgCl_2$ at 37 °C under magnetic stirring. The assembly of α-Syn with each Ssa1p concentration was performed in triplicate. Aliquots (90 μl) were removed at time intervals, spun at 40,000 × *g*, 20 °C, and 20 min in a TL100 tabletop ultracentrifuge (Beckman Coulter). The proteins within the supernatant and pellet fractions were analyzed by SDS-PAGE and quantified following staining/destaining using NIH ImageJ software (available at rsb.info.nih.gov/ij). The nature of the oligomeric species was assessed using a Jeol 1400 transmission electron microscope (Jeol, Ltd.) following adsorption of the samples onto carbon-coated 200-mesh grids and negative staining with 1% uranyl acetate. The images were recorded with a Gatan Orius CCD camera (Gatan).

Cross-linking, SDS-PAGE, and Western Blotting—Cross-linking reactions were carried out with the homobifunctional sulfo-NHS ester cross-linker reagents BS2G-d0/d4 Bis [Sulfosuccinimidyl] glutarate, with a 7.7 Å spacer arm (Pierce, Waltham, MA). α-Syn (100 μM), Hsc70 or Ssa1p (10 μM), or α-Syn and Hsc70 or Ssa1p (100 and 10 μM, respectively) were incubated for 2 h at 37 °C under agitation in 50 mM Tris-HCl, pH 7.5, 150 mM KCl, before dialyzing for 2.5 h at 4 °C against cross-linking buffer (40 mM Hepes-OH, pH 7.5, 75 mM KCl before adding the cross-linker. BS2G (50 mM in dimethyl sulfoxide) was added to give molar ratio 10:1 BS2G:α-Syn and 100:1 BS2G:Hsc70 or Ssa1p. After 30 min at room temperature, the reaction was terminated by addition of ammonium bicarbonate (50 mM). Samples for SDS-PAGE were immediately mixed (v/v) with denaturing buffer and heated at 95 °C. SDS-PAGE was performed in 7.5% tris-tricine polyacrylamide gels following the standard method described by Laemmli (30).

Peptide Preparation—The protein bands corresponding to α-Syn, Hsc70, Ssa1p, and α-Syn after treatment with BS2G, Hsc70, or Ssa1p after treatment with BS2G, and the Hsc70-α-Syn BS2G cross-linked complex and Ssa1p-α-Syn BS2G cross-linked complex were excised from the SDS-PAGE separation. Each protein band was subjected to enzymatic digestion using the Progest robot (Genomic Solutions, Chemsford, MA). Briefly, protein bands were extensively washed with acetronitrile and 25 mM NH_4HCO_3, before reduction and alkylation of cysteine residues in the presence of 10 mM DTT and 55 mM of iodoacetamide. Trypsin (Promega Gold; Promega, Madison, WI) digestion was performed overnight at room temperature in 25 mM NH_4HCO_3. The volume of the trypsin solution (10 ng/μl) was adapted to the size of the protein band excised from the gel (25 μl per 5 mm^3). Peptides were extracted by incubation during 2 h at room temperature after addition of two volumes of 60% CH_3CN, 0.1% HCOOH. The extracted peptides were vacuum dried, dissolved in water and stored at −20 °C until MS analysis.

NanoLC-Linear Ion Trap (LTQ)-Orbitrap Mass Spectrometry Analysis—Tryptic peptide digests were analyzed by nanoLC-MS/MS using an EASY-nLC II high performance liquid chromatography (HPLC) system (Proxeon, Thermo-Scientific, Waltham, MA) coupled to the nanoelectrospray ion source of an LTQ-Orbitrap Velos mass spectrometer (Thermo Scientific). Peptide separation was performed on a reversed-phase C18 nano HPLC column (100 μm inner diameter, 5-μm C18 particles, 15-cm length, NTCC-360/100-5) from Nikkyo Technos (Nikkyo Technos Co., Ltd., Tokyo, Japan). The peptides were loaded at a pressure-dependent flow rate corresponding to a maximum pressure of 200 bars and eluted at a flow rate of 300 nl/min using a gradient of 5 to 35% solvent B for 60 min, followed by a washing step at 100% solvent B. Solvent A was 0.1% formic acid in water, and solvent B was 0.1% formic acid in 100% acetonitrile. NanoLC-MS/MS experiments were conducted in the data-dependent acquisition mode. The mass of the precursors was measured with a high resolution (60,000 full weight at half maximum) in the Orbitrap. The 20 most intense ions, above an intensity threshold of 5000 counts, were selected for CID fragmentation and analysis in the LTQ.

NanoLC-MS/MS data were processed automatically using the Thermo Proteome Discoverer software (version 1.3) and the Sequest search engine with the following chemical modifications: methionine oxidation, cysteine carbamidomethylation, and monolink or loop link modification of lysine residues with BS2G-d0 or BS2G-d4. NanoLC-MS data were further ana-

lyzed as described previously (31). Briefly, nanoLC-MS data were deisotoped using the Decon2LS software (http://omics.pnl.gov/software/Decon2LS.php). The resulting csv files were further analyzed with viper (http://omics.pnl.gov/software/VIPER.php) (32) to identify, within the nanoLC-MS analysis, the d0/d4 peptide pairs corresponding to mass differences of 4.0247 Da as a signature of peptides that reacted with at least one molecule of BS2G-d0/d4. A list of peptide pairs with a maximum mass tolerance of 10 ppm was generated. Mass deviation and peptide elution time were used to filter the list of peptide pairs, corresponding to candidate cross-linked peptides or mono-linked or loop-linked peptides. The list of light and heavy precursor masses was used to identify the BS2G-d0/d4 peptides using GPMAW (33) and XQUEST (34) software. MS/MS spectra of the candidate cross-linked peptides were further analyzed manually to confirm their identification.

RESULTS

Interaction between Hsc70 and Soluble α-Syn—We recently demonstrated that Hsc70 sequesters α-Syn in an assembly incompetent state (18). We show here (Fig. 1*A*) that the Hsc70-α-Syn complex is cross-linked by the homobifunctional NHS-ester BS2G. BS2G reacts with the ϵ-amino group of lysine residues and the α-amino group from protein N termini and, to a lesser extent, with the hydroxyl groups of serine, threonine, and tyrosine residues (35) and has a spacer arm 7.7 Å long. Thus, the residues involved in the interaction within the partner protein complex must be ~7.7 Å away from each other for cross-linking to occur. The affinity of Hsc70 for its client polypeptides is modulated by nucleotides (ATP or ADP). The most efficient sequestering activity was observed for Hsc70 in the absence of nucleotide. Hsc70 inhibits to a lesser extent α-Syn assembly in the presence of ATP (18). This is why cross-linking was performed in the absence of nucleotide. No inhibition α-Syn assembly is observed in the presence of ADP (18). Consistent with that no Hsc70-α-Syn complex with apparent molecular mass of 100 kDa was observed in the presence of BS2G and ADP.

The Interaction between Ssa1p and Soluble α-Syn—In a manner similar to what we observed upon incubation of Hsc70 with α-Syn, when Ssa1p and α-Syn are incubated in the presence of BS2G, an abundant Ssa1p-α-Syn complex with an apparent molecular mass of ~100 kDa forms (Fig. 1*B*), suggesting that Ssa1p binds α-Syn.

The effect of Ssa1p on α-Syn assembly was assessed using a sedimentation assay and electron microscopy (EM). Over time, α-Syn readily assembles into high molecular weight assemblies *in vitro*, which sediment upon centrifugation. Assembly follows a typical sigmoidal pattern, with nucleation, growth, and steady state phases. In the absence of Ssa1p, the nucleation phase of α-Syn at 200 μM is ~200 min. Upon addition of increasing concentrations of Ssa1p, the length of the nucleation phase increases, indicating that the yeast chaperone slows down α-Syn assembly (Fig. 1*C*). EM images of the samples at 1200 min show that there are less fibrils and more non fibrillar oligomeric species upon increasing the concentration of Ssa1p from 0 to 10 μM Ssa1p (Fig. 1*D*). The lag time preceding assembly of α-Syn fibrils in the presence of increasing concentrations

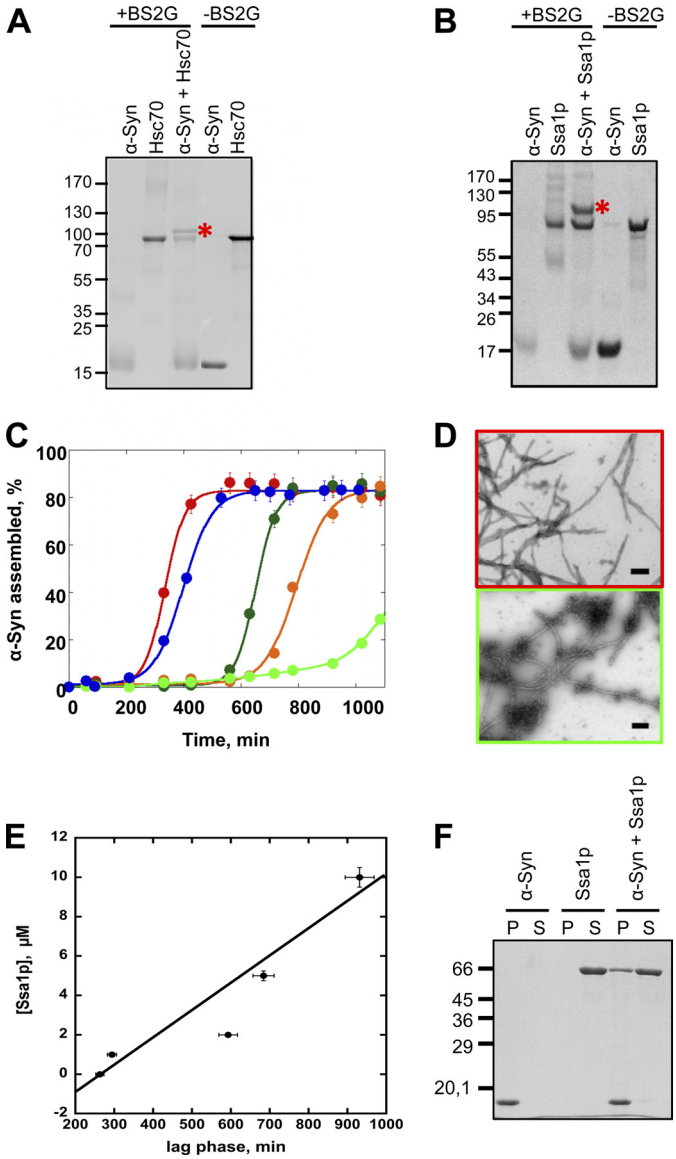

FIGURE 1. **α-Syn-Hsc70 and α-Syn-Ssa1p complex formation.** *A*, SDS-PAGE analysis of cross-linked α-Syn and Hsc70. The reaction products generated upon treatment of α-Syn, Hsc70, and α-Syn in the presence of Hsc70 and the cross-linking agent BS2G were separated on a 7.5% acrylamide SDS-PAGE and stained with Coomassie Blue. *B*, SDS-PAGE analysis of cross-linked α-Syn and Ssa1p. The reaction products generated upon treatment of α-Syn, Ssa1p, and α-Syn in the presence of Ssa1p and the cross-linking agent BS2G were separated on a 7.5% acrylamide SDS-PAGE and stained with Coomassie Blue (*left*). *C*, time courses of α-Syn (200 μM) in the absence (*red*) and the presence of increasing concentrations of Ssa1p: *blue*, 1 μM; *dark green*, 2 μM; *orange*, 5 μM; *light green*, 10 μM. The assembly reactions, performed in triplicate, were monitored by quantifying α-Syn within the pellet and supernatant fractions by SDS-PAGE, as described under "Experimental Procedures." The data were fitted to the equation, $y = a/(1 + \exp(b \times (c - x)))$, where *a* is the proportion of assembled α-Syn at steady state, *c* is the time where 50% of assembly is reached, and *b* is the slope of the exponential growth phase. *D*, negative stained electron micrographs of α-Syn (200 μM) assemblies obtained in the absence (*top*) or presence of 10 μM Ssa1p (*bottom*). *Bar*, 0.2 μm. *E*, the lag time preceding the assembly of a constant α-Syn concentration (200 μM) and increasing Ssa1p concentrations (1–10 μM) depends on Ssa1p concentrations as determined from the assembly reactions presented in *C*. The lag time is plotted as a function of Ssa1p concentration. *F*, SDS-PAGE analysis of the pellet (*P*) and supernatant (*S*) fractions of fibrillar α-Syn (60 μM), Ssa1p (6 μM), and fibrillar α-Syn (60 μM) incubated with Ssa1p (6 μM) for 1 h at 37 °C.

of Ssa1p was measured and plotted as a function of Ssa1p concentration and appeared to increase nearly linearly with increasing Ssa1p concentrations (Fig. 1*E*). These results there-

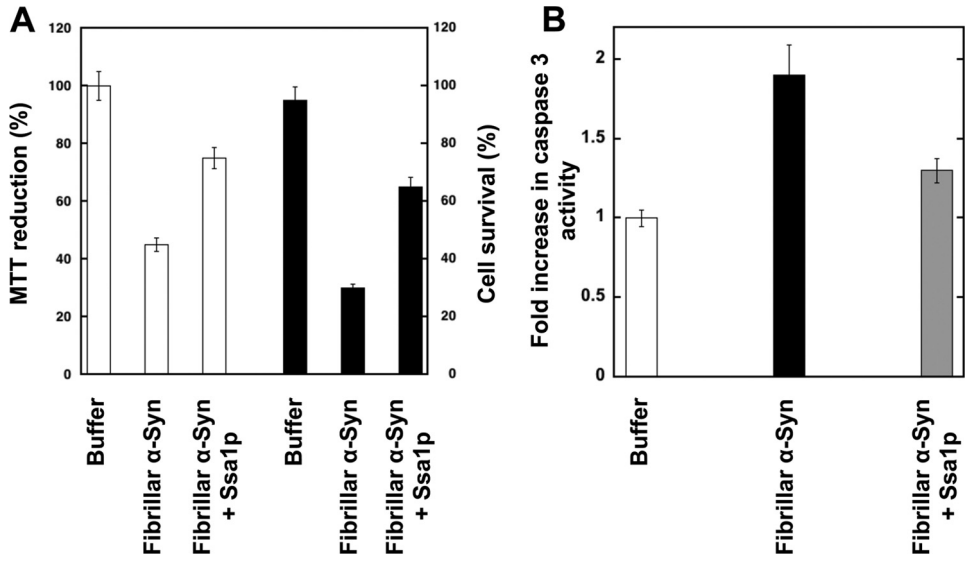

FIGURE 2. **Viability of H-END cells upon exposure to fibrillar α-Syn in the absence or presence of Ssa1p and caspase-3 activation.** Before exposure to cells, fibrillar α-Syn (100 μM) was incubated for 1 h at 37 °C with Ssa1p (25 μM). Fibrillar α-Syn was centrifuged for 20 min at 16,100 × *g*, and the pellet was resuspended in the culture medium to remove unbound Ssa1p. The final protein concentration within the culture medium was 1 μM. *A*, *left axis*, cell viability is expressed as the percentage of 3-(4,5-dimethylthiazol-2-yl)-2,5-diphenyltetrazolium bromide (*MTT*) reduction using cells treated with the same volume of buffer as a reference (100% 3-(4,5-dimethylthiazol-2-yl)-2,5-diphenyltetrazolium bromide reduction) after incubation of the cells with the different proteins for 24 h. The values are mean ± S.E. obtained from three independent experiments. *Right axis*, proportion of murine endothelioma H-END surviving after exposure to fibrillar α-Syn covered or not by Ssa1p. In the latter measurements, cells lifted by 0.5 mM EDTA were incubated for 20 min in suspension in the presence of naked or Ssa1p coated fibrillar-Syn. The cells were then plated on Petri dishes and cultured for 24 h in the presence of added α-Syn. The surviving adherent cells were then lifted by EDTA, and their number was determined in the presence of trypan blue in four independent experiments using a hemocytometer. *B*, caspase-3 activation in H-END cells incubated with 1 μM naked fibrillar α-Syn (*solid bar*) or fibrilar α-Syn pre-incubated with Ssa1p as described above (*gray bar*). Data are shown as fold increase relative to the caspase-3 activity measured in control cells treated with assembly buffer (*white bar*). Data are mean ± S.E. ($n = 3$). *, $p < 0.05$ (Student's *t* test).

fore show that Ssa1p affects α-Syn assembly in a manner similar to Hsc70 (18).

Similarly to Hsc70, Ssa1p also binds to preformed α-Syn fibrils. Indeed, as shown in Fig. 1*F*, Ssa1p is found in the pellet after coincubation with preformed α-Syn fibrils, whereas Ssa1p is in the supernatant of control samples spun under identical conditions in the absence of α-Syn fibrils. Binding of Ssa1p to fibrillar α-Syn reduces significantly the toxicity of α-Syn fibrils as assessed using the MTT assay and cell survival upon treatment of the cells for 24 h with the assemblies (Fig. 2*A*). This parallels a reduced activation of caspase-3 (Fig. 2*B*).

Identification of the Hsc70 or Ssa1p and α-Syn Cross-linked Polypeptides—The analytical strategy used to characterize the polypeptides involved in the Hsc70-α-Syn and Ssa1p-α-Syn interaction was described previously (31) and relies on the use of a mixture of the non-deuterated (d0) and deuterated (d4) forms of BS2G. Untreated, BS2G-treated Hsc70, Ssa1p and α-Syn and the BS2G cross-linked Hsc70-α-Syn and Ssa1p-α-Syn complexes resolved by SDS-PAGE were cleaved by trypsin and the protein sequence coverage determined by the nanoLC-MS/MS analyses described under "Experimental Procedures." The sequence coverage was 94, 98, and 100% for untreated Hsc70, Ssa1p, and α-Syn, respectively, 78, 92, and 100% for Hsc70, Ssa1p, and α-Syn treated with BS2G, respectively, and 100 and 78% for α-Syn and Hsc70 and 73 and 81% for α-Syn and Ssa1p, in the cross-linked Hsc70-α-Syn (Fig. 3*A*) and Ssa1p-α-Syn complexes, respectively (Fig. 3*B*). The modified peptides were detected by MS using the 4.0247 atomic mass unit mass difference conferred by the binding of the nondeuterated or deuterated cross-linkers (36, 37). The exact mass measurements we obtained allowed the identification of all of these peptides using GPMAW (33) and XQUEST (34) software with a mass tolerance of 5 ppm. MS/MS fragmentation mass spectra allowed further unambiguous identification of the cross-linked peptides and the cross-linking sites. Eight Hsc70-α-Syn cross-links were thus identified. The identification of two such cross-linked polypeptides by nanoLC-MS/MS LTQ-Orbitrap analyses is illustrated in Fig. 4. The MS spectra of the quadruple charged Hsc70 494–500-α-Syn 11–21 and triple charged Hsc70 551–561-α-Syn 97–102 cross-links with *m*/*z* 483.5075/484.5139 and 667.6883/669.0295 ion pairs for the BS2G-d0 and BS2G-d4 peptides, are presented in Fig. 4, *A* and *D*, respectively. The LTQ-Orbitrap fragmentation mass spectra of the BS2G-d0 ions with *m*/*z* 483.76 and 668.02 are shown in the *middle panels* of Fig. 4, *B* and *E*. Finally, the α-Syn and Hsc70 sequences of the cross-linked peptides identified through y and b fragment ions are displayed in Fig. 4, *C* and *F*.

As to Ssa1p-α-Syn, 11 cross-links were identified. The identification of two representative cross-linked polypeptides by nanoLC-MS/MS LTQ-Orbitrap analyses are presented in Fig. 5. The MS spectra of the triple charged Ssa1p 491–497-α-Syn 11–21 and Ssa1p 548–567-α-Syn 97–102 cross-links with *m*/*z* 620.3333/621.6749 and the quadruple charged 737.3781/738.3834 ion pairs for the BS2G-d0 and BS2G-d4 peptides, are shown in Fig. 5, *A* and *D*. The LTQ-Orbitrap fragmentation mass spectra of the BS2G-d4 ions with *m*/*z* 621.67 and 738.38 are presented in Fig. 5, *B* and *E*. Finally, the α-Syn and Ssa1p sequences of the cross-linked peptides identified through y and b fragment ions are displayed in Fig. 5, *C* and *F*.

Hsc70- and Ssa1p-α-Synuclein Interaction Interfaces

The list of BS2G cross-linked Hsc70-α-Syn and Ssa1p-α-Syn peptides within the complexes identified following exactly the approach exemplified above is presented in Tables 1 and 2. Cross-links involving Hsc70 494–500, 508–517, 551–561, and 558–569, Ssa1p 445–448, 447–455, 491–497, 498–506, 522–532, 533–547, and 548–567 (Table 1) and α-Syn 7–12, 11–21,

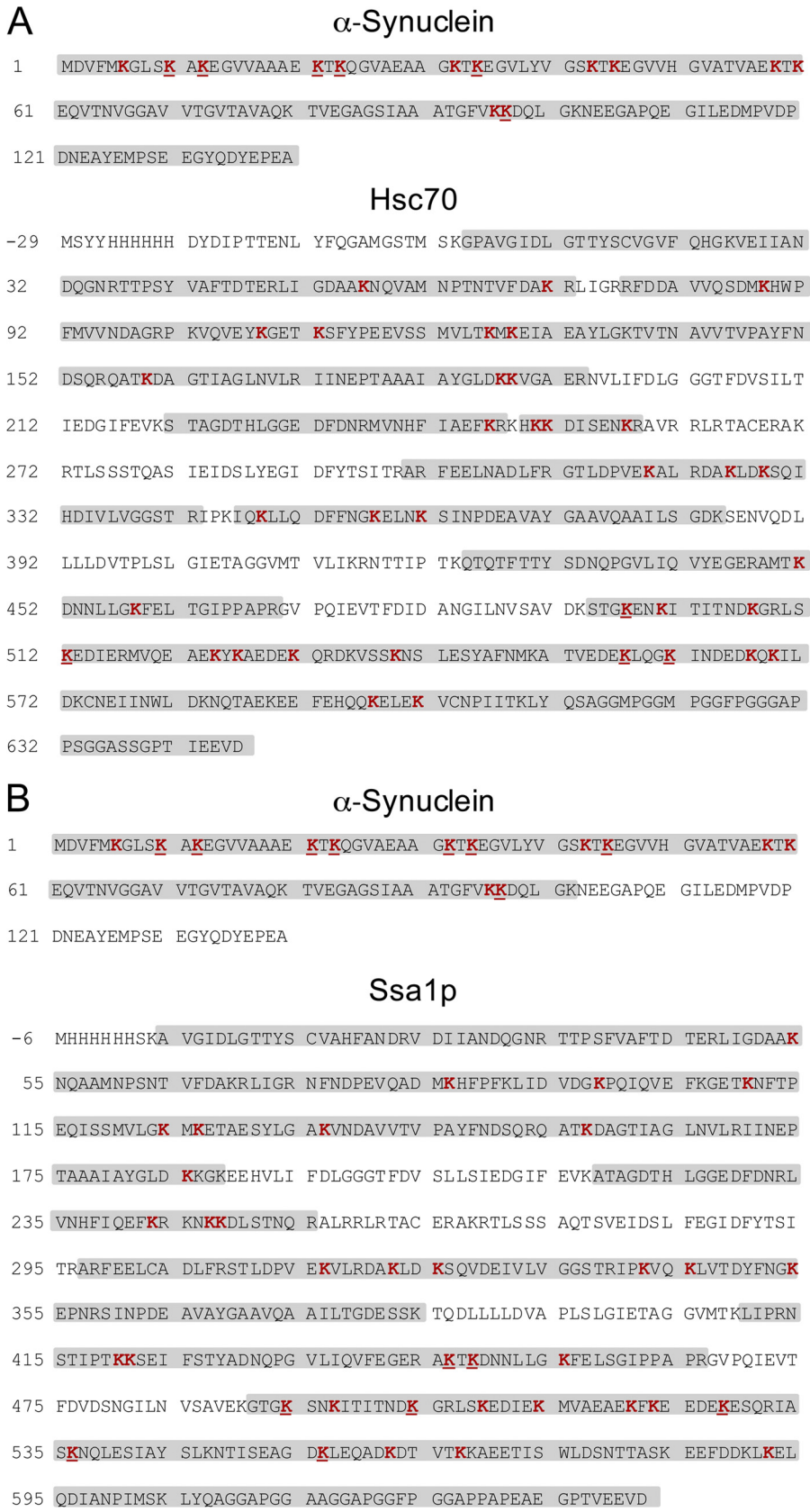

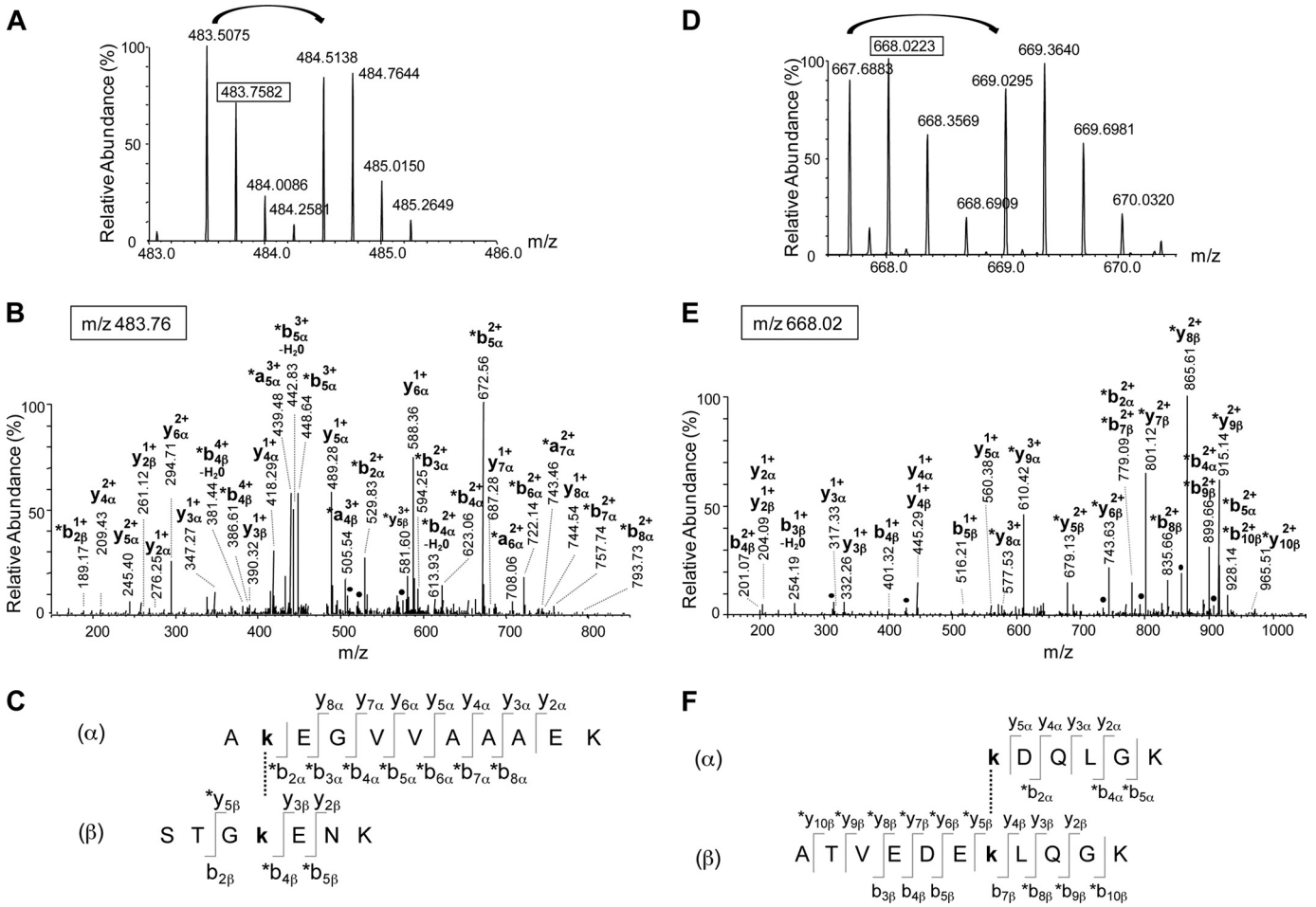

FIGURE 4. **Identification of two cross-links between α-Syn and Hsc70.** *A–C*, identification of the cross-link between peptide 11–21 from α-Syn and peptide 494–500 from Hsc70. *A*, mass spectrum of the quadruple charged cross-linked peptide with *m/z* 483.5075 and 484.5138 for the BS2G-d0 and BS2G-d4 peptides respectively. *B*, fragmentation spectrum of the precursor ion at *m/z* 483.76 corresponding to the second isotope of the BS2G-d0 peptide. The identified fragments and their charge state are indicated. The *asterisks* indicate the fragments with the BS2G-d0 cross-linker. *C*, the identified fragments are indicated on the cross-linked sequences. The α- and β-sequences correspond to the 11–21 α-Syn and the 494–500 Hsc70 peptides, respectively. This cross-link involves residues Lys-12 and Lys-497 from α-Syn and Hsc70, respectively. *D–F*, identification of the cross-link between peptide 97–102 from α-Syn and peptide 551–561 from Hsc70. *D*, mass spectrum of the triple charged cross-linked peptide with *m/z* 667.6883 and 669.0295 for the BS2G-d0 and BS2G-d4 peptides, respectively. *E*, Fragmentation spectrum of the precursor ion at *m/z* 668.02 corresponding to the second isotope of the BS2G-d0 peptide. The identified fragments are indicated, together with their charge state. The *asterisks* indicate the fragments with the BS2G-d0 cross-linker. *F*, the identified fragments are indicated on the cross-linked sequences. The α- and β-sequences correspond to the 97–102 α-Syn and the 551–561 Hsc70 peptides, respectively. This cross-link involves residues Lys-97 and Lys-557 from α-Syn and Hsc70, respectively.

13–23, 22–32, 24–34, 33–43, 44–58, and 97–102 were identified (Table 2). All of the cross-linked lysine residues within Hsc70 (Lys-497, Lys-512, Lys-557, and Lys-561) and Ssa1p (Lys-446, Lys-448, Lys-494, Lys-504, Lys-528, Lys-536, and Lys-556) are situated within the client protein binding domain of the molecular chaperones. None of the lysine residues located within the nucleotide binding domains of the molecular chaperones and exposed at the surface of either Hsc70 or Ssa1p, 27 and 26 lysine residues in total, respectively, were found cross-linked to α-Syn. This strongly suggests that the complexes we identified are not the consequence of unspecific interactions or random encounters. Lysine residues exposure to solvents was estimated using CCP4 (38) solvent accessible surfaces tools (AREAIMOL) using the structural models that we built (see below).

Four lysine residues from α-Syn (Lys-12, Lys-21, Lys-23, and Lys-32) are found cross-linked to Lys-497 from Hsc70. Two additional lysines from α-Syn (Lys-10 and Lys-97) are found either cross-linked to Lys-497 or Lys-512 or to Lys-557 or Lys-561 from Hsc70. Similarly, seven lysine residues from α-Syn (Lys-10, Lys-21, Lys-23, Lys-32, Lys-34, Lys-45, and Lys-97) are found cross-linked to unique lysine residues from Ssa1p (Lys-448, Lys-494, Lys-528, and Lys-556). One additional lysine residue from α-Syn (Lys-12) is found cross-linked to several lysine residues from Ssa1p (Lys-446, Lys-494, Lys-504, and Lys-536).

FIGURE 3. **Primary structure coverage of α-Syn, Hsc70, and Ssa1p obtained following tryptic digestion of the Hsc70-α-Syn (*A*) and Ssa1p-α-Syn (*B*) BS2G cross-linked complex.** The stretches labeled in *gray* correspond to peptides identified by nanoLC-MS/MS analysis. The lysine residues identified as mono-linked or loop-linked are in *red*, and those cross-linked within the Hsc70-α-Syn BS2G complex (*A*) and Ssa1p-α-Syn BS2G (*B*) complex are *underlined*. Sequence coverage was 100% for α-Syn and 75% for Hsc70 and 73% for α-Syn, and 74% for Ssa1p in the Hsc70-α-Syn and Ssa1p-α-Syn BS2G cross-linked complex, respectively. Hsc70 and Ssa1p sequences start at −6, to exclude the His_6 tag and correspond to the exact amino acids numbering of the Hsc70 and Ssa1p sequences.

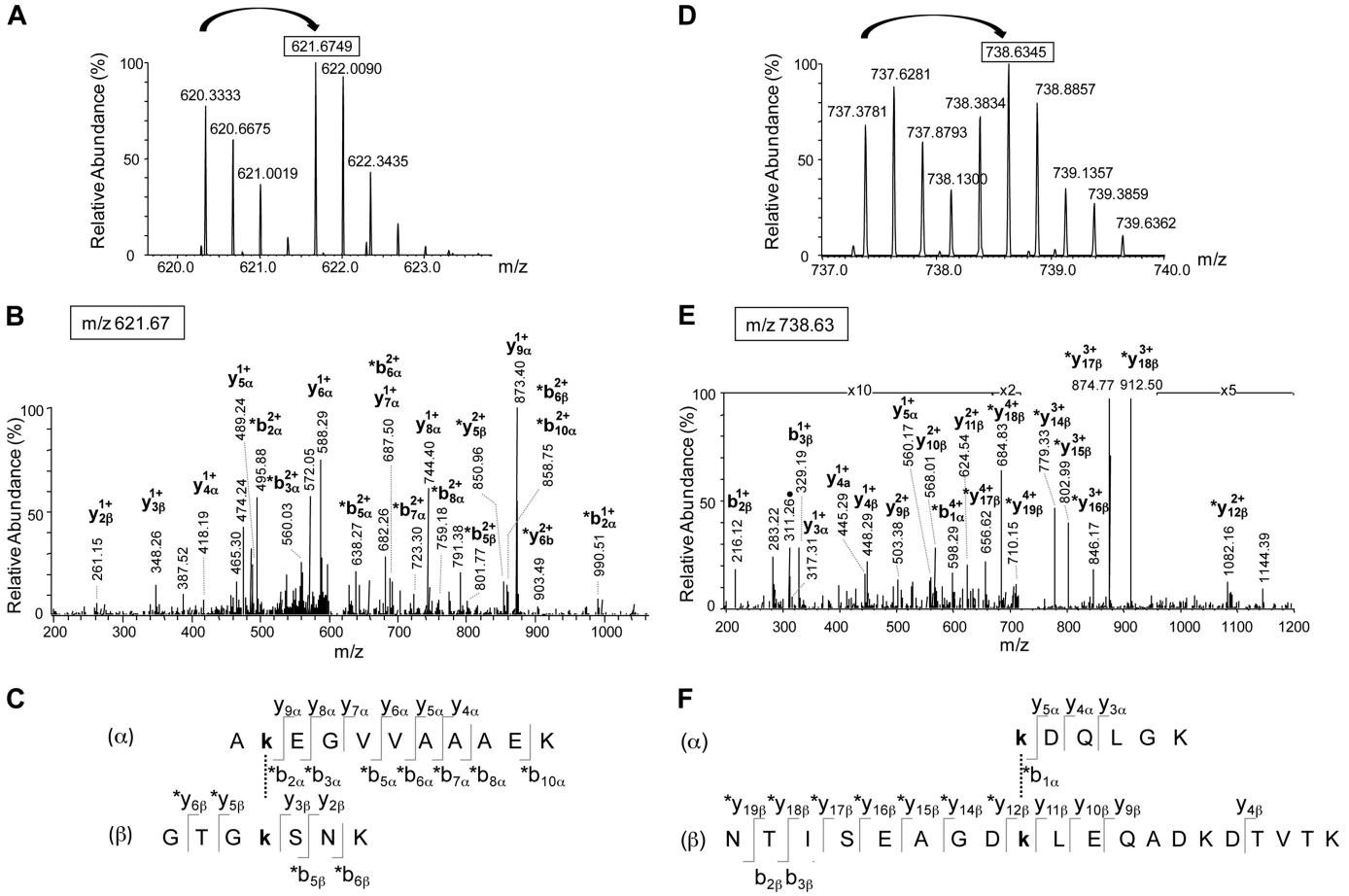

FIGURE 5. **Identification of two cross-links between α-Syn and Ssa1p.** *A–C*, identification of the cross-link between peptide 11–21 from α-Syn and peptide 491–497 from Ssa1p. *A*, mass spectrum of the triple charged cross-linked peptide with *m/z* 620.3333 and 621.6749 for the BS2G-d0 and BS2G-d4 peptides, respectively. *B*, fragmentation spectrum of the precursor ion at *m/z* 621.67 corresponding to the first isotope of the BS2G-d4 peptide. The identified fragments are annotated on the peptide sequence, and their charge states are indicated. The *asterisks* indicate the fragments with the BS2G-d4 cross-linker. *C*, the identified fragments are indicated on the cross-linked sequences. The α- and β-sequences correspond to the 11–21 α-Syn and the 491–497 Ssa1p peptides, respectively. This cross-link involves residues Lys-12 and Lys-494 from α-Syn and Ssa1p, respectively. *D–F*, identification of the cross-link between peptide 97–102 from α-Syn and peptide 548–567 from Ssa1p. *D*, mass spectrum of the quadruple charged cross-linked peptide with *m/z* 737.3781 and 738.3834 for the BS2G-d0 and BS2G-d4 peptides, respectively. *E*, fragmentation spectrum of the precursor ion at *m/z* 738.63 corresponding to the second isotope of the BS2G-d4 peptide. The identified fragments are indicated, together with their charge state. The *asterisks* indicate the fragments with the BS2G-d4 cross-linker. *F*, the identified fragments are indicated on the cross-linked sequences. The α- and β-sequences correspond to the 97–102 α-Syn and the 548–567 Ssa1p peptides, respectively. This cross-link involves residues Lys-97 and Lys-556 from α-Syn and Ssa1p, respectively.

TABLE 1

List of the identified Hsc70-α-synuclein cross-linked peptides

For each identified cross-linked peptide in Hsc70-α-Syn BS2G complexes, the table gives the experimental mass (M exp), the charge state (*z*), the *m/z* ratio for both the BS2G-d0 and the BS2G-d4 peptides, the amino acid segment, the cross-linked lysine residue (XL site), and the amino acid sequence for both the Ssa1p peptide and the α-Syn peptide. DM (ppm) corresponds to the mass deviation between the experimental mass and the theoretical mass, given by XBobCat software (34).

BS2G-d0 peptides			BS2G-d4 peptides			Hsc70 peptide			αSynuclein peptide			ΔM
M exp	*z*	*m/z*	M exp	*z*	*m/z*	Segment	XL site	Sequence	Segment	XL site	Sequence	(ppm)
1460.7821	3	487.9352	1464.8069	3	489.2768	494–500	Lys-497	STG**k**ENK	7–12	Lys-10	GLS**k**AK	0.9
1900.0430	3	634.3555	1904.0687	3	635.6974	508–517	Lys-512	GRLS**k**EDIER	7–12	Lys-10	GLS**k**AK	2.7
1916.9759	4	480.2518	1921.0031	4	481.2586	494–500	Lys-497	STG**k**ENK	22–32	Lys-23	T**k**QGVAEAAGK	2.3
1916.9759	4	480.2518	1921.0031	4	481.2586	494–500	Lys-497	STG**k**ENK	24–34	Lys-32	QGVAEAAG**k**TK	2.3
1929.9987	4	483.5075	1934.0243	4	484.5138	494–500	Lys-497	STG**k**ENK	11–21	Lys-12	A**k**EGVVAAAEK	1.1
1960.0100	3	654.3445	1964.0351	3	655.6862	494–500	Lys-497	STG**k**ENK	13–23	Lys-21	EGVVAAAE**k**TK	0.7
2000.0414	3	667.6883	2004.0650	3	669.0295	551–561	Lys-557	ATVEDE**k**LQGK	97–102	Lys-97	**k**DQLGK	0.6
2198.1515	4	550.5457	2202.1751	4	551.5516	558–569	Lys-561	LQG**k**INDEDKQK	97–102	Lys-97	**k**DQLGK	1.3

We conclude from these observations that α-Syn interacts exclusively with the client binding domain of the molecular chaperones Hsc70 and Ssa1p. We further conclude that α-Syn interacts with a subset of lysines from the client polypeptide binding domain of Hsc70 (four of 25) and Ssa1p (seven of 25). The latter findings highlight the specificity of the interaction between Hsc70 or Ssa1p and α-Syn.

We built a three-dimensional model of Hsc70 using the structures of the ATPase and peptide binding domains, amino acid residues 1–537 of bovine Hsc70 (Uniprot entry P19120), which shares 100% primary structure identity with human Hsc70, and the NMR solution structure of the C-terminal domain (amino acids 537 to 610) of human Hsp70 (Uniprot entry P08107, sharing 69% sequence identity with Hsc70), Pro-

TABLE 2

List of the identified Ssa1p-α-synuclein cross-linked peptides

For each identified cross-linked peptide in Ssa1p-α-Syn BS2G complexes, the table gives the experimental mass (M exp), the charge state (*z*), the *m*/*z* ratio for both the BS2G-d0 and the BS2G-d4 peptides, the amino acid segment, the cross-linked lysine residue (XL site), and the amino acid sequence for both the Ssa1p peptide and the α-Syn peptide. DM (ppm) corresponds to the mass deviation between the experimental mass and the theoretical mass, given by XBobCat software (34).

BS2G-d0 peptides			BS2G-d4 peptides			Ssa1p peptide			α-Synuclein peptide			ΔM
M exp	*z*	*m*/*z*	M exp	*z*	*m*/*z*	Segment	XL site	Sequence	Segment	XL site	Sequence	(ppm)
1613.897	3	538.973	1617.9217	3	540.31451	445–448	Lys-446	A**k**TK	11–21	Lys-12	A**k**EGVVAAAEK	1
1699.946	3	567.6558	1703.9707	3	568.99751	447–455	Lys-448	T**k**DNNLLGK	7–12	Lys-10	GLS**k**AK	0.8
1844.958	3	615.9932	1848.9824	3	617.33474	491–497	Lys-494	GTG**k**SNK	24–34	Lys-32	QGVAEAAG**k**TK	0.7
1857.9783	3	620.3334	1862.0028	3	621.67488	491–497	Lys-494	GTG**k**SNK	11–21	Lys-12	A**k**EGVVAAAEK	0.7
1887.99	3	630.3371	1892.0141	3	631.67864	491–497	Lys-494	GTG**k**SNK	13–23	Lys-21	EGVVAAAE**k**TK	0.4
1966.037	3	656.3528	1970.06135	3	657.69439	491–497	Lys-494	GTG**k**SNK	33–43	Lys-34	T**k**EGVLYVGSK	0.3
2184.174	4	547.0507	2188.1982	4	548.05683	498–506	Lys-504	ITITND**k**GR	11–21	Lys-12	A**k**EGVVAAAEK	0.6
2310.2169	4	578.5615	2314.2416	4	579.56768	491–497	Lys-494	GTG**k**SNK	44–58	Lys-45	T**k**EGVVHGVATVAEK	0.4
2578.2499	4	645.5698	2582.2742	4	646.57583	522–532	Lys-528	FKEEDE**k**ESQR	22–32	Lys-23	T**k**QGVAEAAGK	0.5
2831.5283	4	708.8894	2835.55245	4	709.89539	533–547	Lys-536	IASk**k**NQLESIAYSLK	11–21	Lys-12	A**k**EGVVAAAEK	0.1
2945.4831	4	737.3781	2949.50715	4	738.38406	548–567	Lys-556	NTISEAGD**k**LEQADKDTVTK	97–102	Lys-97	**k**DQLGK	0.1

tein Data Bank codes 1YUW and 2LMG, respectively. The structure of 2LMG was mutated to fit the sequence of Hsc70 and positioned relative to the peptide binding domain using *E. coli* DnaK structure (Uniprot entry P0A6Y8, Protein Data Bank code 1BPR). For Ssa1p, the three-dimensional model was built using the ATPase domain of bovine Hsc70 (Uniprot entry P19120) and the peptide binding domain of *E. coli* DnaK (Uniprot entry P0A6Y8), Protein Data Bank codes 3HSC and 1BPR, respectively. The ATPase domain of bovine Hsc70 and the peptide binding domain of *E. coli* DnaK share 92 and 67% sequence similarity with the corresponding domains of Ssa1p. The three-dimensional models presented in Fig. 6 were used to map Hsc70 and Ssa1p lysine residues involved in interactions with α-Syn. The observation that Lys-12, Lys-21, Lys-23, Lys-32, and Lys-97 from α-Syn are exclusively found within 7.7 Å distance from Lys-497, Lys-557, and Lys-561 from Hsc70, whereas Lys-10 from from α-Syn is found cross-linked with Lys-497 and Lys-512 from Hsc70 strongly suggests that one part of α-Syn is specifically docked to Hsc70 client protein binding site, whereas the other is flexible and capable of interacting with several regions within this site. This conclusion is further strengthened by the finding that Lys-10, Lys-21, Lys-23, Lys-32, Lys-34, Lys-45, and Lys-97 from α-Syn are exclusively cross-linked to Lys-448, Lys-528, and Lys-556 from Ssa1p, respectively, whereas Lys-12 from α-Syn is found cross-linked with Lys-446, Lys-494, Lys-504, or Lys-536 from Ssa1p, suggesting once again that one part of α-Syn is specifically docked to Ssa1p client protein binding site, whereas the other is flexible and capable of interacting with several regions within this site.

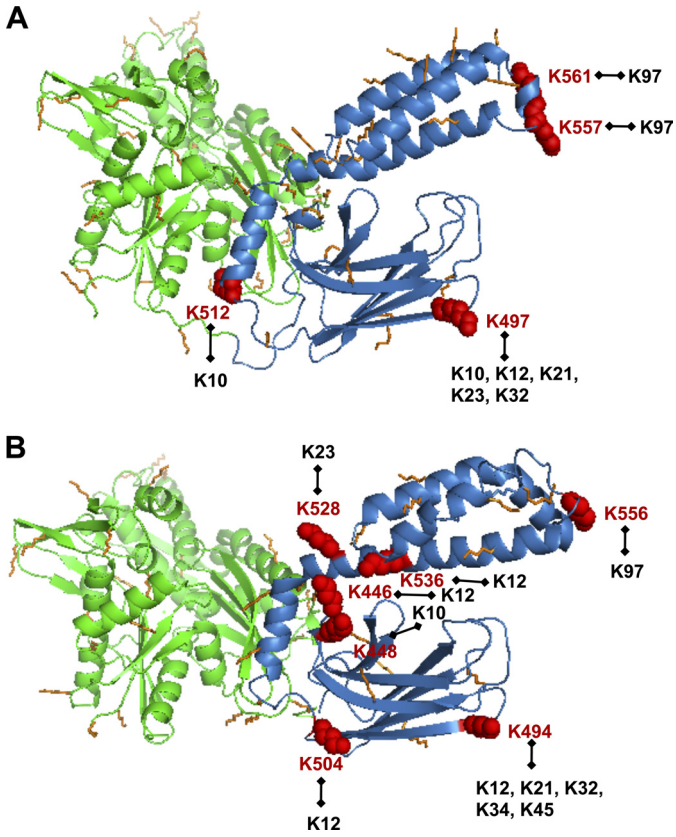

FIGURE 6. **Location of the cross-linked lysines in Hsc70 (*A*) and Ssa1p (*B*).** Lysine residues are depicted as *orange sticks*, and cross-linked lysines are colored in *red*. For each lysine from Hsc70 (*A*) and Ssa1p (*B*) cross-linked to α-Syn in the Hsc70-α-Syn and Ssa1p-α-Syn BS2G complex, the cross-linked lysine residue from α-Syn is indicated in *black*. The Hsc70 and Ssa1p three-dimensional model were built as described in the text. This figure was generated using PyMOL.

DISCUSSION

α-Syn assembly into high molecular weight species is tightly associated to the pathogenesis of PD. We and others previously showed that members of the molecular chaperone family such as Hsc70, Hsp70, and Hsp90 inhibit α-Syn assembly into fibrils *in vitro*, reduce the size of α-Syn aggregates *in vivo*, and protect against α-Syn toxicity (4–6). Extracellular fibrillar α-Syn assemblies have also been shown to be uptaken by cells exposed to these aggregates, to seed the aggregation of endogenous α-Syn, and to propagate from cell-to-cell (4). It has been hypothesized that the latter phenomena might contribute to the progressive spread of aggregated α-Syn throughout the nervous system in synucleinopathies (7, 8). As molecular chaperones sequester α-Syn in an assembly incompetent state and as they reduce the toxicity of fibrils most likely because they change their physicochemical properties upon binding to the fibrils, there is a possibility that they could be effective therapeutic agents in PD (18, 20). We therefore assessed the surface interface between Hsc70 and α-Syn using chemical cross-linking and nanoLC-MS/MS LTQ-Orbitrap analyses to design through future investigations a minimal synthetic molecular chaperone containing what is necessary and sufficient for interacting with α-Syn. Indeed, the thorough identification of client

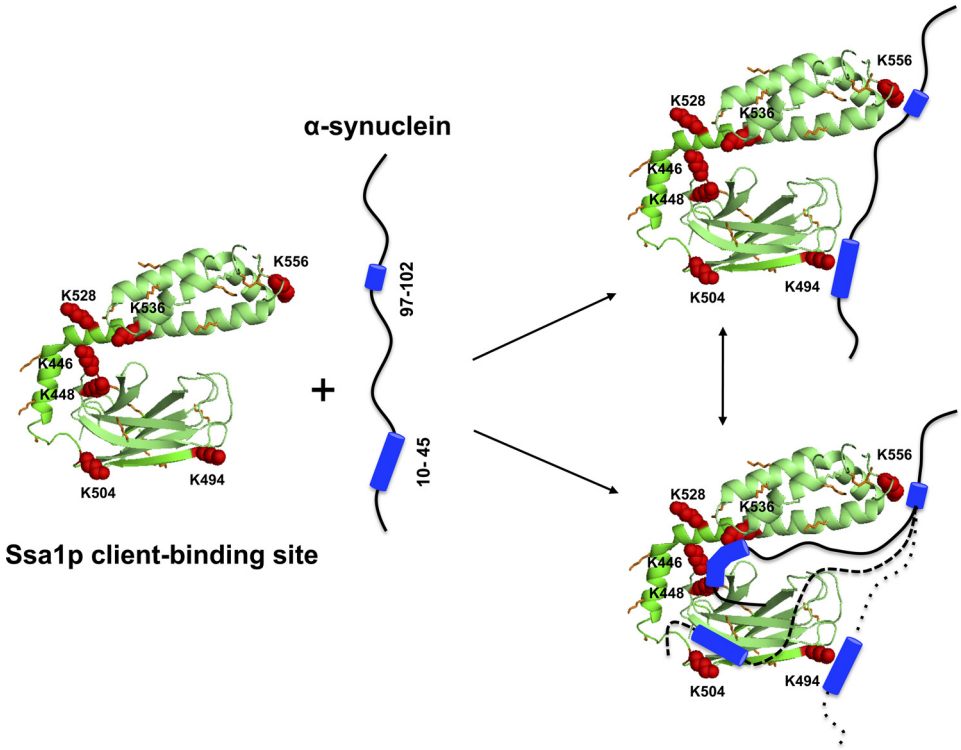

FIGURE 7. **Molecular model for the binding of α-Syn to Ssa1p.** The proposed model is based on the identification of the residues involved in the interaction between the heat shock protein Ssa1p and α-Syn, probed by chemical cross-linking. Lys-10, Lys-21, Lys-23, and Lys-97 from α-Syn are exclusively cross-linked to Lys-448, Lys-528, and Lys-556 from Ssa1p, whereas Lys-12 from α-Syn is found cross-linked with Lys-446, Lys-494, Lys-504, or Lys-536 from Ssa1p. This suggest that after the docking of the regions centered on residues Lys-97 and Lys-556 in α-Syn and Ssa1p, respectively, the N-terminal part of α-Syn establishes interactions with either the back or the bottom tip of the client proteins binding site of Ssa1p. At one stage, Ssa1p appears to bind α-Syn as a tweezer, through the two tips of its client protein binding site.

protein binding sites was successful in designing the GroEL-derived minichaperone that has been shown to have high chaperone activity, independent of the central cavity or allosteric behavior. As the introduction of an endogenous protein or a fragment thereof within the body may evoke an autoimmune response, we also mapped the surface interface between the yeast homologue of Hsc/p70, Ssa1p, and α-Syn.

We show here that α-Syn cross-links to Hsc70 and Ssa1p in the presence of the homobifunctional NHS-ester BS2G to yield Hsc70-α-Syn and Ssa1p-α-Syn complexes with apparent molecular masses of ~100 kDa. α-Syn binds to the client protein binding sites of Hsc70 and Ssa1p. The residues involved in the interaction were identified by nanoLC-MS/MS LTQ-Orbitrap analyses of the tryptic digest of the BS2G cross-linked Hsc70-α-Syn and Ssa1p-α-Syn complexes. The finding that Lys-97 from α-Syn is exclusively found within 7.7 Å distance (the length of BS2G spacer arm) from Lys-557 and Lys-561 from Hsc70 and Lys-556 from Ssa1p which all lie within the lid of the client binding domain of the molecular chaperones, whereas Lys-10, Lys-12, Lys-21, Lys-23, Lys-32, Lys-34, and Lys-45 from α-Syn is found cross-linked with Lys-497 and Lys-512 from Hsc70 and Lys-446, Lys-448, Lys-494, Lys-504, Lys-528, Lys-536, or Lys-556 from Ssa1p strongly suggests that one part of α-Syn is specifically docked to the Ssa1p client protein binding site, whereas the other is flexible and capable of interacting with several regions within this site. Two amino acid stretches within α-Syn located between residues 45 and 97 have hydrophobicity scores equivalent to DNAK client peptide NRLLLTG (Protein Data Bank code 1DKX), allowing them to bind the client binding sites of Hsc70 and Ssa1p. These stretches span residues 50–56 and 69–79 based on Kyte and Doolittle hydrophobicity profiles. The dynamics of α-Syn binding to Hsc70 and Ssa1p allows α-Syn Lys-97 to interact with Hsc70 Lys-557 and Lys-561 and Ssa1p Lys-556, whereas the rest of the N-terminal part of α-Syn interacts with either the back or the bottom tip of the client protein binding site of Hsc70 and Ssa1p leading to a scheme where Ssa1p and Hsc70 appear to bind α-Syn as a tweezer, through the two tips of their client protein binding site (Figs. 6 and 7).

Our findings together with those where antibodies directed against α-Syn assembly are used (39, 40) lay the foundations for a therapeutic strategy targeting soluble α-Syn and inhibiting its assembly into fibrils or modifying the surface properties of fibrils in such a way that they become less toxic and/or intercellular propagation is perturbed. Indeed, our results are invaluable for the design of future therapeutic tools in PD as we describe within a molecular chaperone client binding domain what is necessary and possibly sufficient to bind α-Syn. This should allow the engineering of a subset of the client binding site of molecular chaperones from the Hsc/p70 family that bind α-Syn in a manner similar to the entire chaperone or with increased affinity. The agent should ideally be based on a non-human protein, as small as possible while still effective, to limit the chance of autoantibodies being produced leading to autoimmune disease, similar to that seen when the drug levodopa was first introduced to alleviate PD symptoms (22–25).

Acknowledgments—This work benefited from the platform "Identification and Characterization of Proteins by Mass Spectrometry" (SICaPS), a joint IMAGIF/Centre de Recherche de Gif and Federative Research Institute Genomes, Transcriptomes, Proteomes facility. We thank David Cornu for help in automatic tryptic digestion.

REFERENCES

1. Uversky, V. N., Li, J., Bower, K., and Fink, A. L. (2002) Synergistic effects of pesticides and metals on the fibrillation of α-synuclein: Implications for Parkinson disease. *Neurotoxicology* **23,** 527–536
2. Ross, C. A., and Smith W. W. (2007) Gene-environment interactions in Parkinson disease Parkinsonism. *Relat. Disord.* **13,** S309–15
3. Spillantini, M. G., Schmidt, M. L., Lee, V. M., Trojanowski, J. Q., Jakes, R., and Goedert, M. (1997) α-Synuclein in Lewy bodies. *Nature* **388,** 839–840
4. Hansen, C., Angot, E., Bergström, A. L., Steiner, J. A., Pieri, L., Paul, G., Outeiro, T. F., Melki, R., Kallunki, P., Fog, K., Li, J. Y., and Brundin, P. (2011) α-Synuclein propagates from mouse brain to grafted dopaminergic neurons and seeds aggregation in cultured human cells. *J. Clin. Invest.* **121,** 715–725
5. Desplats, P., Lee, H. J., Bae, E. J., Patrick, C., Rockenstein, E., Crews, L., Spencer, B., Masliah, E., and Lee, S. J. (2009) Inclusion formation and neuronal cell death through neuron-to-neuron transmission of α-synuclein. *Proc. Natl. Acad. Sci. U.S.A.* **106,** 13010–13015
6. Volpicelli-Daley, L. A., Luk, K. C., Patel, T. P., Tanik, S. A., Riddle, D. M., Stieber, A., Meaney, D. F., Trojanowski, J. Q., and Lee, V. M. (2011) Exogenous α-synuclein fibrils induce Lewy body pathology leading to synaptic dysfunction and neuron death. *Neuron* **72,** 57–71
7. Braak, H., Del Tredici, K., Rüb, U., de Vos, R. A., Jansen Steur, E. N., and Braak, E. (2003) Staging of brain pathology related to sporadic Parkinson disease. *Neurobiol. Aging* **24,** 197–211
8. Brundin, P., Melki, R., and Kopito, R. (2010) Prion-like transmission of protein aggregates in neurodegenerative diseases. *Nat. Rev. Mol. Cell Biol.* **11,** 301–307
9. Pieri, L., Madiona, K., Bousset, L., and Melki, R. (2012) Fibrillar α-synuclein and huntingtin exon 1 assemblies are toxic to the cells. *Biophys. J.* **102,** 2894–2905
10. Vabulas, R. M., Raychaudhuri, S., Hayer-Hartl, M., and Hartl, F. U. (2010) Protein folding in the cytoplasm and the heat shock response. *Cold Spring Harb. Perspect. Biol.* **2,** a004390
11. Hartl, F. U., and Hayer-Hartl, M. (2009) Converging concepts of protein folding *in vitro* and *in vivo*. *Nat. Struct. Mol. Biol.* **16,** 574–581
12. Luk, K. C., Mills, I. P., Trojanowski, J. Q., and Lee, V. M. (2008) Interactions between Hsp70 and the hydrophobic core of α-synuclein inhibit fibril assembly. *Biochemistry* **47,** 12614–12625
13. Danzer, K. M., Ruf, W. P., Putcha, P., Joyner, D., Hashimoto, T., Glabe, C., Hyman, B. T., and McLean, P. J. (2011) Heat-shock protein 70 modulates toxic extracellular α-synuclein oligomers and rescues trans-synaptic toxicity. *FASEB J.* **25,** 326–336
14. Dedmon, M. M., Christodoulou, J., Wilson, M. R., and Dobson, C. M. (2005) Heat shock protein 70 inhibits α-synuclein fibril formation via preferential binding to prefibrillar species. *J. Biol. Chem.* **280,** 14733–14740
15. Huang, C., Cheng, H., Hao, S., Zhou, H., Zhang, X., Gao, J., Sun Q. H., Hu, H., and Wang, C. C. (2006) Heat shock protein 70 inhibits α-synuclein fibril formation via interactions with diverse intermediates. *J. Mol. Biol.* **364,** 323–336
16. Klucken, J., Shin, Y., Masliah, E., Hyman, B. T., and McLean, P. J. (2004) Hsp70 reduces α-synuclein aggregation and toxicity. *J. Biol. Chem.* **279,** 25497–25502
17. Richter, K., Haslbeck, M., and Buchner, J. (2010) The heat shock response: Life on the verge of death. *Mol. Cell.* **40,** 253–266
18. Pemberton, S., Madiona, K., Pieri, L., Kabani, M., Bousset, L., and Melki, R. (2011) Hsc70 protein interaction with soluble and fibrillar α-synuclein. *J. Biol. Chem.* **286,** 34690–34699
19. Roodveldt, C., Bertoncini, C. W., Andersson, A., van der Goot, A. T., Hsu, S. T., Fernández-Montesinos, R., de Jong, J., van Ham, T. J., Nollen, E. A., Pozo, D., Christodoulou, J., and Dobson, C. M. (2009) Chaperone proteostasis in Parkinson disease: Stabilization of the Hsp70/α-synuclein complex by Hip. *EMBO J.* **28,** 3758–3770
20. Pemberton, S., and Melki, R. (2012) The interaction of Hsc70 protein with fibrillar α-synuclein and its therapeutic potential in Parkinson disease. *Commun. Integr. Biol.* **5,** 94–95
21. Witt, S. N. (2010) Hsp70 molecular chaperones and Parkinson disease. *Biopolymers* **93,** 218–228
22. Cotzias, G. C., and Papavasiliou, P. S. (1969) Autoimmunity in patients treated with levodopa. *JAMA* **207,** 1353–1354
23. Linström, F. D., Liedén, G., and Enström, M. S. (1977) Dose-related levodopa-induced haemolytic anaemia. *Ann. Intern. Med.* **86,** 298–300
24. Territo, M. C., Peters, R. W., and Tanaka, K. R. (1973) Autoimmune hemolytic anemia due to levodopa therapy. *JAMA* **226,** 1347–1348
25. Wanamaker, W. M., Wanamaker, S. J., Celesia, G. G., and Koeller, A. A. (1976) Thrombocytopenia associated with long term levodopa therapy. *JAMA* **235,** 2217–2219
26. Ghee, M., Melki, R., Michot, N., and Mallet, J. (2005) PA700, the regulatory complex of the 26 S proteasome, interferes with α-synuclein assembly. *FEBS J.* **272,** 4023–4033
27. McClellan, A. J., and Brodsky, J. L. (2000) Mutation of the ATP-binding pocket of SSA1 indicates that a functional interaction between Ssa1p and Ydj1p is required for post-translational translocation into the yeast endoplasmic reticulum. *Genetics* **156,** 501–512
28. Bradford, M. M. (1976) A rapid and sensitive method for the quantitation of microgram quantities of protein utilizing the principle of protein-dye binding. *Anal. Biochem.* **72,** 248–254
29. Melki, R., Carlier, M. F., Pantaloni, D. (1990) Direct evidence for GTP and GDP-Pi intermediates in microtubule assembly. *Biochemistry* **29,** 8921–8932
30. Laemmli, U. K. (1970) Cleavage of structural proteins during the assembly of the head of bacteriophage T4. *Nature* **227,** 680–685
31. Redeker, V., Bonnefoy, J., Le Caer, J. P., Pemberton, S., Laprévote O., and Melki, R. (2010) A region within the C-terminal domain of Ure2p is shown to interact with the molecular chaperone Ssa1p by the use of cross-linkers and mass spectrometry. *FEBS J.* **277,** 5112–5123
32. Zimmer, J. S., Monroe, M. E., Qian, W. J., Smith, R. D. (2006) Advances in proteomics data analysis and display using an accurate mass and time tag approach. *Mass Spectrom. Rev.* **25,** 450–482
33. Peri, S., Steen, H., and Pandey, A. (2001) GPMAW–a software tool for analyzing proteins and peptides. *Trends Biochem. Sci.* **26,** 687–689
34. Rinner, O., Seebacher, J., Walzthoeni, T., Mueller, L. N., Beck, M., Schmidt, A., Mueller, M., and Aebersold, R. (2008) Identification of cross-linked peptides from large sequence databases. *Nat. Methods* **5,** 315–318
35. Mädler, S., Bich, C., Touboul, D., Zenobi, R. (2009) Chemical cross-linking with NHS esters: A systematic study on amino acid reactivities. *J. Mass Spectrom.* **44,** 694–706
36. Seebacher, J., Mallick, P., Zhang, N., Eddes, J. S., Aebersold, R., and Gelb, M. H. (2006) Protein cross-linking analysis using mass spectrometry, isotope-coded cross-linkers, and integrated computational data processing. *J. Proteome Res.* **5,** 2270–2282
37. Maiolica, A., Cittaro, D., Borsotti, D., Sennels, L., Ciferri, C., Tarricone, C., Musacchio, A., and Rappsilber, J. (2007) Structural analysis of multiprotein complexes by cross-linking, mass spectrometry, and database searching. *Mol. Cell Proteomics* **6,** 2200–2211
38. Potterton, E., Briggs, P., Turkenburg, M., and Dodson, E. (2003) A graphical user interface to the CCP4 program suite. *Acta Crystallogr. D Biol. Crystallogr.* **59**, 1131–1137
39. Näsström, T., Gonçalves, S., Sahlin, C., Nordström, E., Screpanti Sundquist, V., Lannfelt, L., Bergström, J., Outeiro, T. F., and Ingelsson, M. (2011) Antibodies against α-synuclein reduce oligomerization in living cells. *PLoS One* **6,** e27230
40. Masliah, E., Rockenstein, E., Mante, M., Crews, L., Spencer, B., Adame, A., Patrick, C., Trejo, M., Ubhi, K., Rohn, T. T., Mueller-Steiner, S., Seubert, P., Barbour, R., McConlogue, L., Buttini, M., Games, D., and Schenk, D. (2011) Passive immunization reduces behavioral and neuropathological deficits in an α-synuclein transgenic model of Lewy body disease. *PLoS One* **6,** e19338